

Final Report

ULTRAFILTRATION FOR XANTHAN PURIFICATION AND SEPERATION FEASIBILITY

Hannah Nisonson

Bioprocess Engineering Laboratory  
Agricultural & Biological Engineering  
West Lafayette, IN 47907

MM

March 30, 2018

## Summary

*Xanthomonas campestris* is a bacterial species that produces the commercially important polysaccharide xanthan by process of fermentation (Garcia, & Ochoa, 2000). Xanthan gum's industrial importance comes from its versatility in that it may be used as a suspending, stabilizing, or emulsifying agent (Lo, Yang, & Min, 1996). The purification process of xanthan from fermentation broth requires a great amount of alcohol for precipitation and equally large amounts of energy for recovery distillation purposes (Lo, Yang, & Min, 1996). To separate xanthan gum from the fermentation broth by removing larger impurities such as lysed *X. campestris* cells, ultrafiltration using a membrane with a molecular weight cut-off of 500,000 daltons operating under cross-flow conditions is a proposed method.

A series of separation steps are needed to concentrate the singular product for separating the solute (xanthan) from the solution given. Unpurified xanthan was fed into the ultrafiltration unit through the peristaltic pumping system. The unit then separated the particles in the stream based on size and permeability of the membrane. Two streams then left the unit, one going to the purified xanthan reservoir being the permeate stream, and the other going back to the unpurified xanthan reservoir (retentate stream). This retentate was fed back into the system to be re-filtered. Over time concentration of xanthan in the retentate should have increased along with a decrease of concentration in the permeate.

Cross-flow filtration arrangement in ultrafiltration for xanthan should not escape through the membrane into the purified collection solution, causing the increase in concentration in retentate. Yet, while the data is too sporadic to observe if this is true, many other constants to test the success and purification of the ultrafiltration process for *Xanthomonas campestris*. The retention coefficient (R), an important parameter used to numerically quantify the selectivity of the membrane used to filtrate xanthan, fell around  $0.80 \leq R \leq 1.0$  meaning the membrane was selective to xanthan. Permeate flux takes accounts for other membrane qualities such as pore size distribution, pore density, membrane porosity, etc. (Doran, 2012). Two operating regions should be considered when analyzing  $J_v$  in a membrane filtration system – pressure-controlled & mass-transfer controlled operation (Doran, 2012). Based on Figure 5, mass-transfer control was observed considering the linear effect permeate flux has on transmembrane pressure making the two independent from each other. Permeate flux, while being defined by the flow rate across the permeate over the area of the membrane, may also be defined empirically as a function of permeate concentration ( $C_p$ ), transmembrane pressure ( $\Delta P$ ), and pumping flow rate (Q). Looking at the theoretical and experimental results, transmembrane pressure ( $\Delta P$ ), permeate concentration ( $C_p$ ), and pumping rate (Q), all have an absolute value of less than one, meaning their effect on  $J_v$  is not linear (Lo, Yang, & Min, 1996).

## **Introduction**

The commercially important polysaccharide xanthan is produced by the bacterial species *Xanthomonas campestris* through process of fermentation (Garcia, & Ochoa, 2000). After fermentation, xanthan gum is present in a solution containing bacterial cells. The xanthan must be separated from the broth to eventually perform bioencapsulation. Ultrafiltration is a membrane process that is similar to reverse osmosis. Whether being pressure driven or mass-transfer driven, solvent and occasionally small molecules pass through a membrane and are collected as permeate. Large molecules won't pass through the membrane and recovered in a retentate stream (Geankopolis, 2013).

Many parameters are used to determine characteristics of the ultrafiltration process. Retention coefficient is defined for the purpose of determining efficiency and selectivity of the membrane. Further more, permeate flux analysis provides tremendous insight into the feasibility of ultrafiltration for xanthan purification. More insight can be found by evaluating both the analytical equation for permeate flux defined by permeate flow rate over cross sectional area and the empirical equation of flux as a function of pressure, concentration and pump.

## **Theory/Basic Principles**

Membranes are usually thin, porous sheets of material that have the ability to separate solid particles from a fluid-solid solution. This is usually done by using force to move the fluid through a filter medium or a filter cloth. This medium or cloth will catch the large/solid particles from passing along with the fluid. Using a vacuum or increasing the pressure to make the fluid pass through the membrane at a faster rate can expedite filtration (Doran, 2012).

Filtration regarding a fermentation standpoint is where cell solids get trapped on a filter cloth and build up to form a porous cake, while liquid in the fermentation solution passes through the cloth. Filtration focuses on the separating, concentration, and purification of products in regards to cells, cell debris, protein concentration, virus removal, etc. Microfiltration, ultrafiltration, and reverse osmosis are all specific examples of membrane filtration (Doran, 2012). There are several more that are used in bioprocessing such as dialysis and osmosis but those are not controlled by a change in pressure.

Membrane filtration usually occurs in either a cross flow manner where the direction of flow is parallel to the membrane or a conventional dead end flow there the direction is perpendicular to the membrane (Doran, 2012). When a particle is large enough to be blocked by a filter cake, fluid can either be pumped or pulled through said filter. Operating principles behind filtration are best described by particles being

separated from a solute by being forced to pass through a membrane. Membrane filtration theory, the idea behind main operating principles, helps to determine the rate of filtration – as it is a function of change in pressure, filter area, volume of filtrate, total mass of the solid, filtrate viscosity, and various resistances (Doran, 2012).

Selectivity is an important parameter to evaluate the viability of membrane filtration operations. It is the ability of the membrane to select among particles in suspension or through the criteria of size. Selectivity can be quantified by a variable known as the retention coefficient (R) as seen by Equation 1, in which  $C_R$  is the solute concentration in the retentate and  $C_P$  is the solute concentration in the permeate (Doran, 2012).

$$R = \frac{C_R - C_P}{C_R} \quad (1)$$

Retention coefficient values should range from zero to one; with one being the membrane was fully permeable to the xanthan ( $C_P = 0$ ) and zero being the membrane was impermeable to the solute ( $C_R = C_P$ ). The correlation coefficient for the separation of lysed cells from xanthan in water should be closer to one in hopes that most of the xanthan was filtered out through the retentate.

Effectiveness of membrane performance is mainly determined by permeate flux ( $J_v$ ). One way flux is quantified is flow rate per area of the membrane as seen represented by Equation 2, where  $F_p$  is the flow rate through the permeate and A is the surface area of the membrane (Doran, 2012).

$$J_v = \frac{F_p}{A} \quad (2)$$

Flux is a major contributor to operating pressure at low pressure, but at higher pressures, it has no correlation with membrane pressure (Doran, 2012). This concept also helps to determine if the reaction runs as “pressure-controlled” or “mass-transfer controlled” (Doran, 2012). Furthermore, permeate flux should have a negative relationship with cell concentration, so with higher cell concentration, permeable flux is decreasing. Permeate flux can also be characterized empirically as seen in Equation 3, where the constants a, b, and c are determined from logarithmic plots of permeate flux ( $J_v$ ), transmembrane pressure ( $\Delta P$ ), xanthan concentration in permeate ( $C_P$ ), and pumping flow rate (Q) (Lo, Yang, & Min, 1996).

$$J_v = 3.51 \times 10^{-5} \Delta P^a C_p^b Q^c \quad (3)$$

Equation 3 may be used to predict permeate flux characteristics for different combinations of the other variables (Lo, Yang, & Min, 1996).

## Experimental

To separate the solute (xanthan) from the solution, a series of separation steps are needed to concentrate the singular product. Figure 1 outlines the ultrafiltration of xanthan using cross flow techniques.

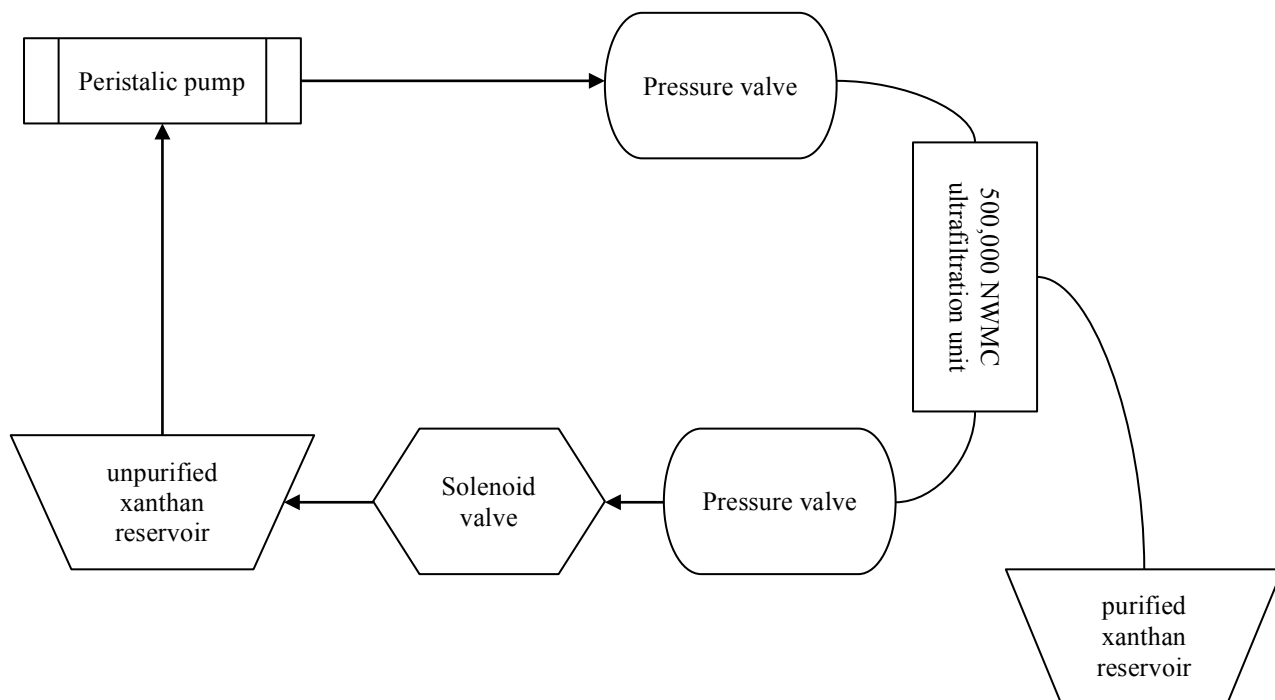


**Figure 1.** A schematic diagram of the membrane ultrafiltration process to separate xanthan from a fermentation solution for purification. Unpurified xanthan was fed into the ultrafiltration unit through the peristaltic pumping system. The unit then separated the particles in the stream based on size and permeability of the membrane. Two streams then left the unit, one going to the purified xanthan reservoir being the permeate stream, and the other going back to the unpurified xanthan reservoir (retentate stream). This retentate was fed back into the system to be re-filtered.

A 3:1 ratio of hydrochloric acid and water to zero and increasing xanthan stock solutions were used to create the xanthan calibration curve as well as calibrate the spectrophotometer. The calibration curve for xanthan can be seen in Figure 2 of Appendix A. The peristaltic pumping system was calibrated by collecting water in a graduated cylinder while simultaneously recording the time it took to collect. Figure 3 in Appendix A displays the pumping flow rate calibration curve. Calculating flow rate from that can be seen in Equation 4.

$$\text{flow rate} = \frac{\text{volume of liquid collected}}{\text{time to collect liquid}} \quad (4)$$

Changing the independent variables – pumping flow rates and transmembrane pressure – to acquire the corresponding values – permeate flow rate, and xanthan concentration in permeate & retentate – generates the data needed to analyze pumping efficiency and characteristics. Altering the pump setting, which ranged from settings 2 to 10, varied pumping flow rate. In addition, transmembrane pressure was changed with increments of 2 starting with 2 psi going all the way up to 10 psi and measured using pressure gauges that can be seen in Figure 1. Permeate flow rate was then measured using a graduated cylinder and stopwatch and subsequently calculated using the formula seen in Equation 4. Permeate and retentate samples were collected at each pressure and pump setting to be diluted, inverted with sulfuric acid, and read in the spectrophotometer. Data was collected for multiple trials; however, retentate was not collected for all the trials at higher pump settings and pressures due to no liquid being released from the pumping equipment.

### **Presentation & Discussion of Results**

As previously stated in Theory and Basic Principles, the retention coefficient (R) is an important parameter used to numerically quantify the selectivity of the membrane used to filtrate xanthan. Not all membranes have ideal and identical pore widths, and as a result, some solutes may be present in both permeate and retentate post filtration. Retention coefficient, R, was quantified using Equation 1. In addition, averages were grouped together and plotted against transmembrane pressure as illustrated in Figure 4. Error bars were also fit to the data showing its wide variability.

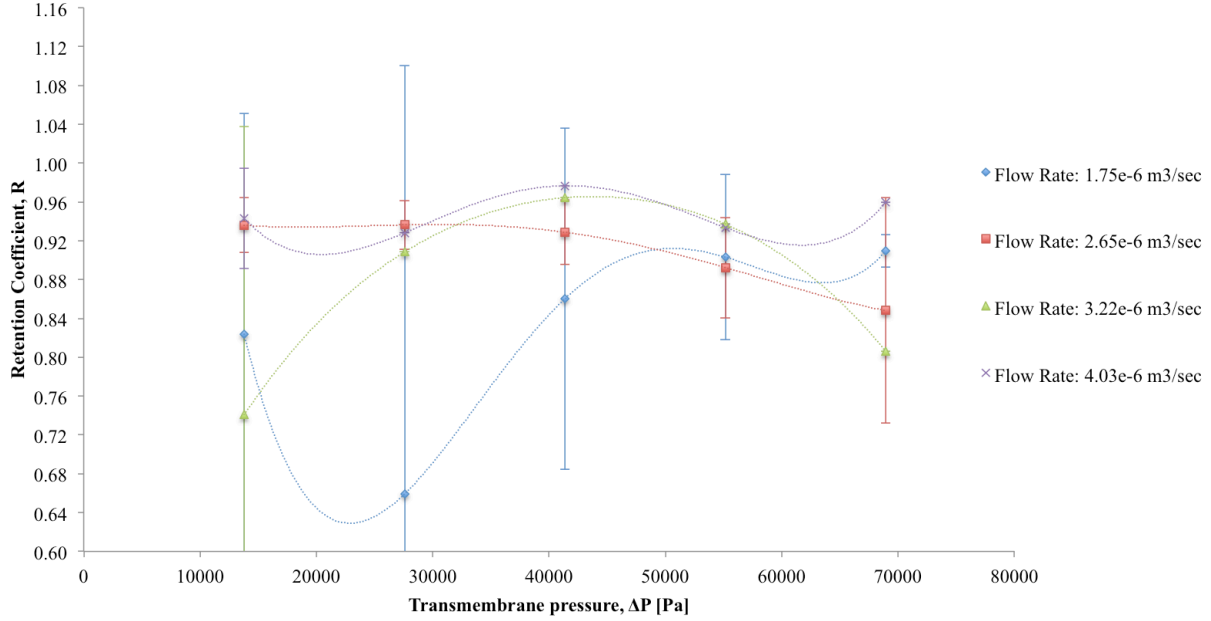


**Figure 4.** Retention Coefficient –  $R$  [-] – compared to transmembrane pressure –  $\Delta P$  [Pa] – at different pumping rates –  $Q$  [ $\text{m}^3/\text{sec}$ ]. Error bars on the graph show large variability in data. There is very little to no relationship between retention coefficient ( $R$ ) and transmembrane pressure ( $\Delta P$ ) because all the data points seem to be randomly dispersed with no particular trend. However, in accordance to pumping flow rate ( $Q$ ), there seems to be a slight increase in retention coefficient with increases in flow rate.

Retention coefficients  $\pm 2$  points away from the standard deviation were excluded from the data set and are not represented graphically. An example of how to calculate retention coefficient based off of xanthan concentrations in permeate and retentate can be found in sample calculations of Appendix B.

An analysis of Figure 4 and the calculated results shows that most of the retention coefficients fall around  $0.80 \leq R \leq 1.0$  meaning the membrane used performed as, if not close to, an ideal membrane. There were some outliers beyond 2 points of the standard deviation, however, those were removed to more accurately observe relationships between the parameters. There is little correlation to be seen between pressure and retention coefficient. Yet, as pumping flow rate increases, a slight visual increase in retention coefficient was observed.

Membranes are characterized by other important properties in addition to retention coefficient, such as the rate of filtration per unit area, also known as permeate flux ( $J_v$ ). Permeate flux takes accounts for other membrane qualities such as pore size distribution, pore density, membrane porosity, etc. (Doran, 2012). Different flux's calculated using Equation 2 were plotted against transmembrane pressures at different pumping flow rates, as seen in Figure 5. Each of the data sets is denoted by different colored markers and lines to show linear trends.

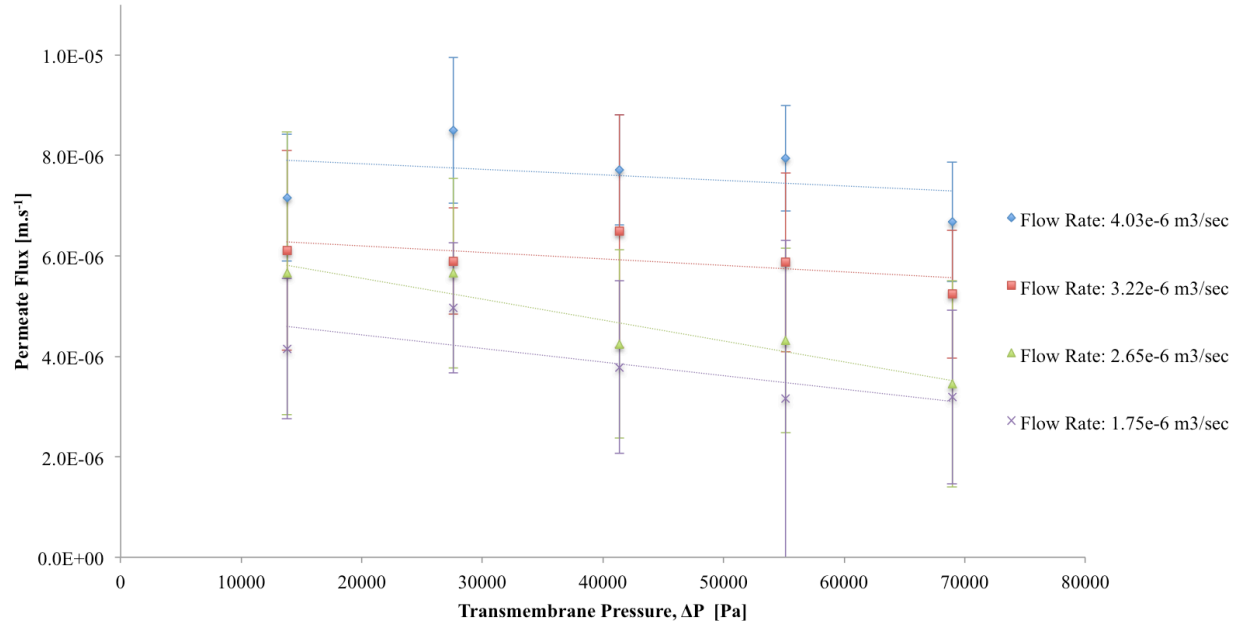


**Figure 5.** The relation between permeate flux –  $J_v$  [ $\text{m}^3 \cdot \text{m}^{-2} \cdot \text{s}^{-1}$ ] – transmembrane pressure –  $\Delta P$  [Pa] – at different pumping rates –  $Q$  [ $\text{m}^3/\text{sec}$ ]. Error bars on the graph show large variability in data. Slight trend lines show low slopes in a downward direction, otherwise the trend lines show very little correlation between transmembrane pressure ( $\Delta P$ ) and permeate flux ( $J_v$ ). Looking at pumping flow rate ( $Q$ ), permeate flux ( $J_v$ ) increases as pumping flow rate increase giving the two a proportional relationship.

Cross flow fluid operating conditions were used to develop relationships between permeate flux and analogous parameters. Analyzing Figure 5, shows that transmembrane pressure,  $\Delta P$ , has very little influence on permeate flux,  $J_v$ , concluded by looking at the low slope linear trend lines fit to the data. Pressure differences exerted across a membrane,  $\Delta P$ , are a principle driving force for membrane filtration. With that said, two operating regions should be considered when analyzing  $J_v$  in a membrane filtration system – pressure-controlled & mass-transfer controlled operation (Doran, 2012). Pressure-controlled operations will result in flux being dependent on pressure represented by an exponential curve upward on a graph. Reversely, mass-transfer control will have a linear effect on a graph of permeate flux and transmembrane pressure because the two would be independent from each other. Visually, the linearity of the trend lines leads to the conclusion of a mass-transfer controlled operation. Following the other relationship expressed in Figure 5, pumping rate consistently increases as permeate flux increases. This is to be expected as permeate flow rate is partially controlled by pumping flow rate leading to the conclusion that cross-flow velocity is dependent on permeate flux as well as the pumping rate action.

Permeate flux, while being defined by the flow rate across the permeate over the area of the membrane ( $650 \text{ cm}^2$ ), may also be defined empirically as a function of permeate concentration ( $C_p$ ), transmembrane pressure ( $\Delta P$ ), and pumping flow rate ( $Q$ ), as seen in Equation 3 (Lo, Yang, & Min, 1996). The natural



log of averages for all parameters listed above were taken and plotted against natural log of permeate flux as shown in Figure 6. Extrapolating the slope of the linear fit for each of these graphs gives the experimental empirical constants for Equation 3. A summary of experimental constants and theoretical constants are laid out in Table 1 of Appendix A.

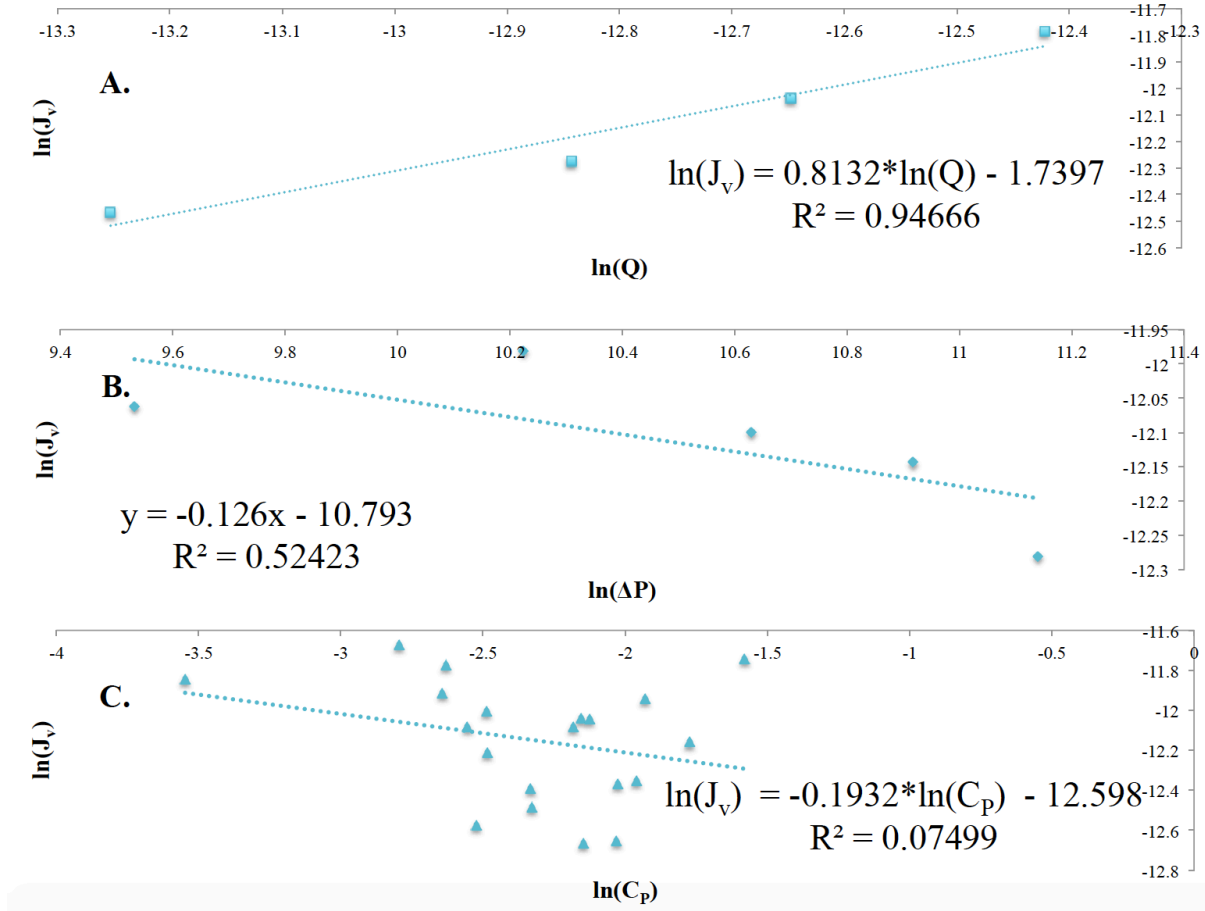


**Figure 6.** Logarithmic plot showing the relationships between  $\ln(\text{permeate flux} - J_v)$  and **A.**  $\ln(\text{pumping rate} - Q)$ , **B.**  $\ln(\text{transmembrane pressure} - \Delta P)$ , & **C.**  $\ln(\text{permeate xanthan concentration} - C_p)$ . Linear trend lines were fit to each set of data points. The slope of the trend lines determines the coefficients of the empirical equation for permeate flux as seen by Equation 3. The fit on graph A. shows a positive slope and a highly correlated fit. However, the trend lines on graph's B. & C. show a negative slope and low correlation as corresponding to the  $R^2$  values, graph C. more so. A summary of the determined slopes compared to the literature values are seen in Table 1.

Looking at Figure 6, graph A. shows a positive slope and a highly correlated fit with an  $R^2$  value of 0.946. However, the trend lines on graph's B. & C. show a negative slope and low correlation as the  $R^2$  values being 0.524 for graph B and 0.075 for C. Equation 5 gives the relationship between determined empirical values, while Equation 6 is the theoretical mathematical model for permeate flux (Lo, Yang, & Min, 1996).

$$J_v = 3.51 \times 10^{-5} \Delta P^{-0.126} C_p^{-0.193} Q^{0.813} \quad (5)$$

$$J_v = 3.51 \times 10^{-5} \Delta P^{0.25} C_p^{-0.64} Q^{0.32} \quad (6)$$

Both these models are used to predict permeate flux through a combination of parameters. Looking at the theoretical and experimental results, transmembrane pressure ( $\Delta P$ ), permeate concentration ( $C_p$ ), and pumping rate ( $Q$ ), all have an absolute value of less than one, meaning their effect on  $J_v$  is not linear (Lo, Yang, & Min, 1996). Experimental transmembrane pressure coefficient compared to theoretical has a negative value instead of being positive, meaning increases of pressure with permeate flux was not seen in the data. As for xanthan concentration in permeate or pumping rate, conversely, the magnitude of the empirical constant values for  $C_p$  and  $Q$  are significantly off from theoretical ( $C_p$  being smaller and  $Q$  being larger). Most of the error and low correlation between parameters was a result of large variations in data.

### Conclusions & Recommendations

Ultrafiltration feasibility for xanthan purification was proven to be successful based on trends found in the figures. As a consequence, the following can be drawn from collected data. The way cross-flow filtration is arranged, xanthan should not escape through the membrane into the purified collection solution, causing the increase in concentration in retentate. The retention coefficient ( $R$ ) for the most part, according to Figure 4, fell around  $0.80 \leq R \leq 1.0$ , with an outlier of 0.6, coming to the conclusion that the membrane was selective to xanthan and  $C_p \approx 0$  in comparison to xanthan concentrations in retentate. When looking at membrane filtration, the two operating regions in question are pressure-controlled & mass-transfer controlled operation. Based on Figure 5, mass-transfer control was observed considering the linear effect permeate flux has on transmembrane pressure making the two independent from each other. This also means flux is largely unaffected by transmembrane pressure. While being defined by the flow rate across the permeate over the area of the membrane, flux can be defined as a function of permeate concentration ( $C_p$ ), transmembrane pressure ( $\Delta P$ ), and pumping flow rate ( $Q$ ). Equation 5 and Equation 6 show vast differences in the magnitude of empirical constants, yet only transmembrane pressure is observed in the opposite direction than expected. Looking at the theoretical and experimental results, transmembrane pressure, permeate concentration, and pumping rate, all have an absolute value of less than one, making their effect on permeate flux non linear. With filtration being mass-transfer controlled, pressure with a most cost-effective rate should be used, considering pressure has little to no effect effectiveness of the process.

The collected data indicates ultrafiltration is the viable process for purification of xanthan. Conversely, improvements can be made to make the process more efficient and effective overall. More efficient and accurate measuring equipment should be used to measure flow rates for both pump and permeate to remove any source of human error.

## Nomenclature

A	Area of membrane	[m <sup>2</sup> ]
a	Empirical constant	[-]
b	Empirical constant	[-]
C <sub>p</sub>	[Xanthan] of the permeate Stream	[g/L]
C <sub>R</sub>	[Xanthan] of the retentate Stream	[g/L]
c	Empirical constant	[-]
F <sub>p</sub>	Volumetric Flow rate of the permeate stream	[m <sup>3</sup> /sec]
J <sub>v</sub>	Permeate Flux	[m <sup>3</sup> .m <sup>-2</sup> /sec]
ΔP	Transmembrane Pressure	[Pa]
Q	Pumping rate	[m <sup>3</sup> /sec]
R	Retention Coefficient	[-]

## Literature Cited

- Doran, P. M. (2013). *Bioprocess Engineering Principles*. Academic Press. Retrieved from <https://books.google.com/books?id=wZSylDhgEXMC&pgis=1>
- Garcia-Ochoa, F., Santos, V.E., Casas J.A., Gómez E. (2000). Xanthan gum: production, recovery, and properties, *Biotechnology Advances*, vol. 18, no. 7, pg. 549-579
- Geankoplis, C. J. (2003). Principles of momentum transfer and applications. In *Transport processes and separation process principles: (includes unit operations)* (4th ed., pp. 121-234). Upper Saddle River, NJ: Prentice Hall Professional Technical Reference.
- Lo, Y. M., Yang, S. T., & Min, D. B. (1996). Kinetic and feasibility studies of ultrafiltration of viscous xanthan gum fermentation broth, *Journal of Membrane Science*

## Appendix A

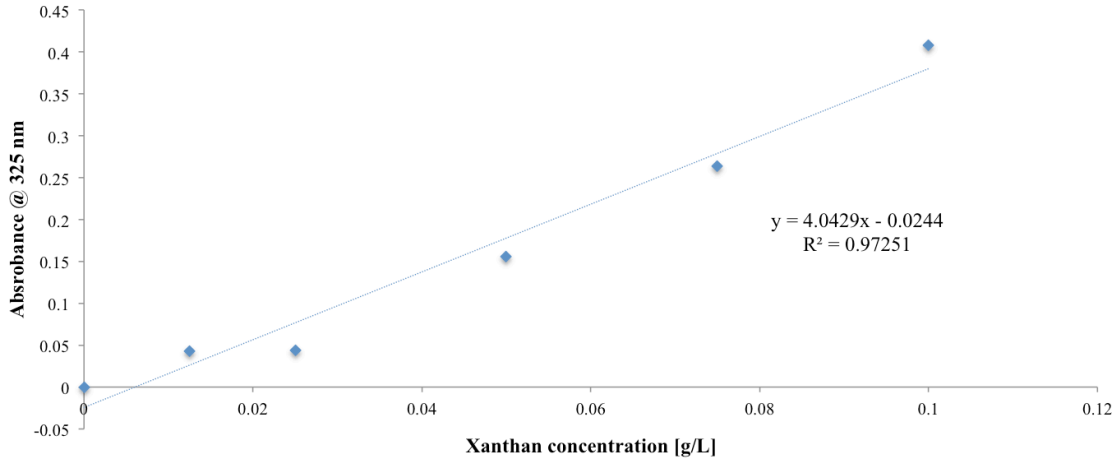


**Figure 2.** Calibration curve for xanthan concentration [g/L] plotted against absorption at 325 nm wavelength. Following the positive correlation between the two, absorbance increases with xanthan concentration.  $R^2$  is 0.97251, which is high enough to presume a strong correlation. An example of how to convert absorbance into xanthan concentration can be found in sample calculations of Appendix B.

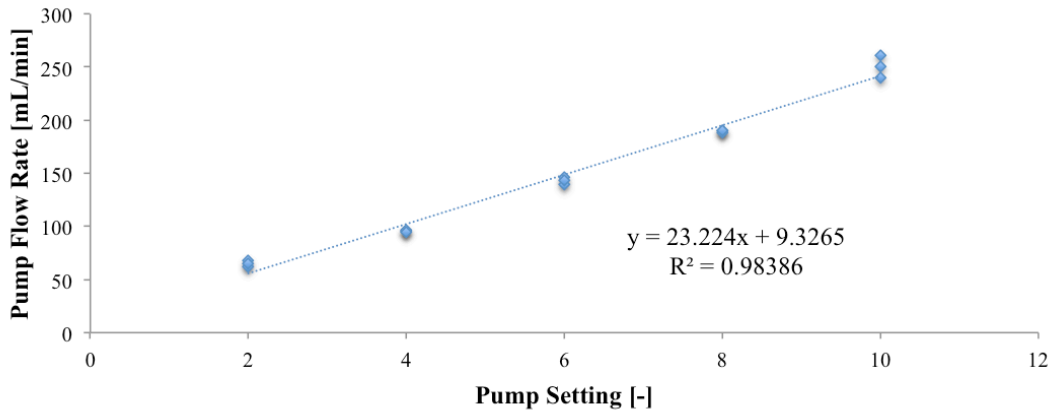


**Figure 3.** Calibration curve for the pump setting [-] when measured against pumping flow rate. There is an obvious positive relationship between setting and flow rate, as the setting increased, pump flow rate also increased.  $R^2$  is 0.98386 which very high, indicating a strong correlation.

**Table 1.** Comparison of graphically determined and theoretical values of the permeate flux equation as seen in Equation 3. Theoretical values came from *Kinetic and feasibility studies of ultrafiltration of viscous xanthan gum fermentation broth* written by Yang Lo, Shang Yang, and David Min. Each of the determined values for the empirical constants were extrapolated from logarithmic plots of permeate flux and the corresponding parameters represented in Figure 6. Values for experimental were rounded to the thousands place.

Parameter	Empirical Constant	Experimental Values	Theoretical Values
$\Delta P$	a	-0.126	0.25
$C_P$	b	-0.193	-0.64
Q	c	0.813	0.32

## Appendix B

### SAMPLE CALCULATIONS

- ① Retention Coefficient,  $R$  [-]  
 concentration of xanthan in permeate,  $C_p$   
 concentration of xanthan in retentate,  $C_R$

$$R = \frac{C_R - C_p}{C_R} \quad \begin{array}{l} C_p = 0.0186 \text{ g/L} \\ C_R = 0.374 \text{ g/L} \end{array}$$

$$R = \frac{0.374 - 0.0186}{0.374} = \boxed{0.950}$$

- ② Calculating permeate flux,  $J_v$  [ $\text{m}^3/\text{s}$ ]

$$J_v = \frac{F_p}{A} \quad \begin{array}{l} F_p = \text{flow rate of permeate} \\ A = \text{cross sectional area of membrane} \end{array}$$

$$F_p = 10.395 \frac{\text{mL}}{\text{min}} \Rightarrow 10.395 \times 1.666 \times 10^{-8} \Rightarrow 1.73 \times 10^{-7} \frac{\text{m}^3}{\text{s}}$$

$$A = 650 \text{ cm}^2 \Rightarrow 0.065 \text{ m}^2$$

$$J_v = 1.73 \times 10^{-7} \frac{\text{m}^3}{\text{s}} \cdot \frac{1}{0.065 \text{ m}^2} = \boxed{2.67 \times 10^{-6} \text{ m/s}}$$

- ③ Calibration curve - converting absorbance to concentration

eqn. from Figure 2 of Appendix A

$$y = 4.0429x - 0.0244$$

permeate absorbance = 0.039

$$0.039 = 4.0429x - 0.0244$$

$$\boxed{x = 0.0036113 \text{ g/L}} - C_p$$

retentate absorbance = 0.202

$$0.202 = 4.0429x - 0.0244$$

$$x = 0.04392$$

x20 (6/L of dilution  
with  $\text{H}_2\text{SO}_4 + \text{H}_2\text{O}$ )

$$\boxed{x = 0.87858 \text{ g/L}} - C_R$$